MIT Libraries | DSpace@MIT

MIT Open Access Articles

The Sensitivity of Latent Heat Flux to Changes in the Radiative Forcing: A Framework for Comparing Models and Observations

Massachusetts Institute of Technology

The Sensitivity of Latent Heat Flux to Changes in the Radiative Forcing: A Framework for Comparing Models and Observations

JONATHAN M. WINTER AND ELFATIH A. B. ELTAHIR

Massachusetts Institute of Technology, Cambridge, Massachusetts

(Manuscript received 27 March 2009, in final form 2 October 2009)

ABSTRACT

A climate model must include an accurate surface physics scheme in order to examine the interactions between the land and atmosphere. Given an increase in the surface radiative forcing, the sensitivity of latent heat flux to available energy plays an important role in determining the energy budget and has a significant impact on the response of surface temperature.

The Penman–Monteith equation is used to construct a theoretical framework for evaluating the climatology of evapotranspiration and the sensitivity of latent heat flux to available energy. Regional Climate Model version 3 coupled to Integrated Biosphere Simulator (RegCM3–IBIS); RegCM3 with its native land surface model, Biosphere–Atmosphere Transfer Scheme 1e (RegCM3–BATS1e); and Flux Network (FLUXNET) micrometeorological tower observations are compared and contrasted using the developed methodology.

RegCM3–IBIS and RegCM3–BATS1e simulate the observed sensitivity of latent heat flux to available energy reasonably well during the summer on average; however, there are significant variations in the monthly values. Additional information provided by the physically based Penman–Monteith framework is employed for identifying deficiencies and guiding improvements in models, allowing calibration of both the climatology of evapotranspiration and the sensitivity of latent heat flux to available energy.

1. Introduction

Whether prescribed as an explicit climate sensitivity or calculated using multiple parameterizations, the response of the surface to changes in the atmosphere is uncertain. One uncertainty in particular, the sensitivity of latent heat flux to an increase in available energy, is especially salient as it directly impacts the effect of climate change on surface temperature. Climate change is likely to accelerate the hydrologic cycle, leading to increased global evapotranspiration and precipitation. In areas where the increase in evapotranspiration significantly exceeds that of precipitation, drought conditions will become more common. This could have extensive impacts on the entire world community if the newly created droughts occur in the midwestern United States or southern Europe, regions of substantial agricultural productivity.

Given an increase in available energy, by what relative magnitudes should climate models increase fluxes of latent and sensible heat? Are the responses of all models similar? If the responses are different, which one is correct? And if it is correct, is it for the right reason? To answer these questions, a thorough understanding of both the climatology and sensitivity of the surface energy budget is needed.

A framework based on the Penman–Monteith equation is developed to identify deficiencies in model predictions of the climatology of evapotranspiration and the response of latent heat flux to an increase in surface radiation. The theoretical sensitivity of latent heat flux to available energy is calculated by taking the partial derivative of the Penman–Monteith formulation of evapotranspiration with respect to available energy. The theoretical sensitivity is shown to be primarily dependent on the ratio of surface resistance to aerodynamic resistance, both of which are calculated to gain additional insight into model performance. Figure 1 illustrates the influence of surface resistance and aerodynamic resistance on both the climatology of evapotranspiration (λE) and the sensitivity of latent heat flux to available energy $\partial \lambda E / \partial A$. Many combinations of resistances can produce a specific latent heat flux; however, to capture both the correct climatology and sensitivity, only one combination of surface resistance and aerodynamic resistance is valid. Therefore,

Corresponding author address: Jonathan M. Winter, MIT Bldg. 48-216, 15 Vassar St., Cambridge, MA 02139.
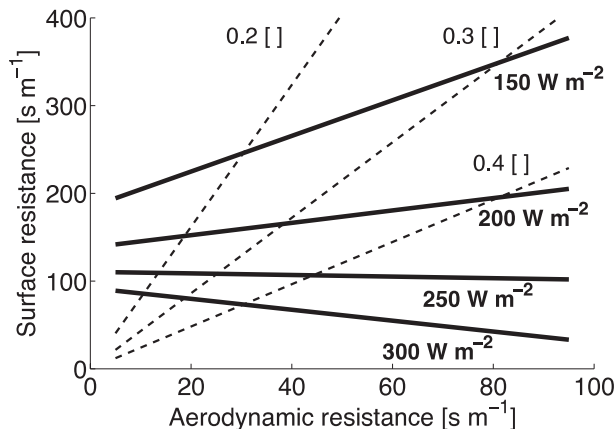E-mail: jwinter@mit.edu

FIG. 1. The relationship between surface and aerodynamic resistance and latent heat flux (solid lines, values in bold) and sensitivity of latent heat flux to available energy (dashed lines) derived using the Penman–Monteith equation. The slope of the saturation vapor pressure–temperature relationship, vapor pressure deficit, and available energy are assumed to be constant values of 150 Pa °C^{-1}, 1500 Pa, and 350 W m^{-2}, respectively.

tuning a model to produce the right climatology alone is not adequate to simulate the response of an ecosystem to a changing atmosphere. The analysis proposed below addresses this problem.

2. Penman–Monteith framework

The Penman–Monteith equation was used to develop a consistent framework for comparing models and observations:

$$\lambda E = \frac{\Delta A + \dfrac{\rho c_p}{r_a}(e_{sat} - e)}{\Delta + \gamma\left(1 + \dfrac{r_s}{r_a}\right)}, \qquad (1)$$

where λE is the latent heat flux, Δ is the slope of the saturation vapor pressure–temperature relationship, A is the available energy, ρ is the mean air density, c_p is the specific heat of air, r_a is the aerodynamic resistance, $(e_{sat} - e)$ is the vapor pressure deficit, γ is the psychometric constant, and r_s is the surface resistance (Shuttleworth 1979).

To examine the characteristics of different surface physics models, all variables except r_s were acquired for each simulation and observational dataset. The Penman–Monteith equation was then used to calculate an implied surface resistance, creating a uniform framework capable of comparing models of varying complexity as well as observations. In addition to r_s, r_a was carefully analyzed because of its strong influence on the partitioning of available energy between latent and sensible heat.

Since r_s and r_a are the two primary variables of interest, the partial derivative of the Penman–Monteith equation was taken with respect to each:

$$\frac{\partial \lambda E}{\partial r_s} = \frac{-\Delta A r_a \gamma - \rho c_p \gamma(e_{sat} - e)}{(\Delta r_a + \gamma r_a + \gamma r_s)^2}, \qquad (2)$$

$$\frac{\partial \lambda E}{\partial r_a} = \frac{\Delta A r_s \gamma - \rho c_p \Delta(e_{sat} - e) - \rho c_p \gamma(e_{sat} - e)}{(\Delta r_a + \gamma r_a + \gamma r_s)^2}. \qquad (3)$$

Equation (2) shows that an increase in surface resistance suppresses latent heat flux. However, the effect of an increase in aerodynamic resistance is not immediately apparent. Both positive and negative terms exist in Eq. (3), so the response of latent heat flux to a change in r_a is dependent on the relative values of the variables describing the current system state:

$$r_s \uparrow \Rightarrow \lambda E \downarrow \quad r_a \uparrow \Rightarrow \lambda E \downarrow \quad \text{or} \quad \lambda E \uparrow. \qquad (4)$$

The sensitivity of the Penman–Monteith equation to available energy is

$$\frac{\partial \lambda E}{\partial A} = \frac{\Delta}{\Delta + \gamma\left(1 + \dfrac{r_s}{r_a}\right)}. \qquad (5)$$

From Eq. (5), it is clear that

$$r_s \uparrow \Rightarrow \frac{\partial \lambda E}{\partial A} \downarrow \quad r_a \uparrow \Rightarrow \frac{\partial \lambda E}{\partial A} \uparrow. \qquad (6)$$

3. Model and dataset description

Regional Climate Model version 3 (RegCM3) is a three-dimensional, sigma-coordinate, hydrostatic, compressible, primitive equation regional climate model originally developed at the National Center for Atmospheric Research (NCAR) and currently maintained at the International Centre for Theoretical Physics (Pal et al. 2007). Integrated Biosphere Simulator (IBIS) is a dynamic global vegetation model that uses a modular, physically consistent framework to perform simulations of water, energy, and carbon fluxes (Foley et al. 1996). The coupling of IBIS to Regional Climate Model version 3 (RegCM3–IBIS) introduced several key advantages to RegCM3, most notably vegetation dynamics, plant competition, and explicit modeling of soil/plant biogeochemistry. However, multiple errors were identified in RegCM3–IBIS, including a significant warm bias and an overestimation of surface shortwave radiation incident, net longwave radiation, and sensible heat flux (Winter et al. 2009).

Several improvements were made to RegCM3–IBIS to address these deficiencies. The overestimation of surface

shortwave radiation incident was reduced by updating the optical properties of water vapor, including background aerosols, and using the Arakawa–Schubert closure assumption for the Grell parameterization of convection. Updated extinction coefficients for water vapor were obtained from NCAR Community Atmosphere Model 3 (Collins et al. 2006). In addition, a cropland plant functional type based on the work of Kucharik and Brye (2003) was added to RegCM3–IBIS to better represent the current vegetation cover of the midwestern United States.

RegCM3–IBIS and RegCM3 with its native surface physics model, Biosphere–Atmosphere Transfer Scheme 1e (RegCM3–BATS1e) were evaluated at two sites where extensive Flux Network (FLUXNET) observations are available. FLUXNET is a network of over 400 micrometeorological tower sites that provides eddy covariance measurements of carbon, water vapor, and energy fluxes between the land surface and atmosphere (Baldocchi et al. 2001). Bondville, Illinois (40.0°N, 88.3°W) is an agricultural site with an annual rotation between soybeans (1998) and corn (1997, 1999). Little Washita Watershed (35.0°N, 98.0°W) is a grassland located near Chickasha, Oklahoma. The data used in this analysis are derived from the Marconi Conference Gap-Filled Flux and Meteorology Dataset (Falge et al. 2005). It is important to acknowledge that errors exist in the FLUXNET observations of latent heat flux and sensible heat flux. Twine et al. (2000) found that uncertainty in the surface energy budget ranged from 10% to 30%, while uncertainty in measuring available energy was approximately 10%. To address errors in the measurements of latent and sensible heat, the methodology of Twine et al. (2000) was used to close the energy budget of FLUXNET observations. Specifically, the ground heat flux was subtracted from the net radiation to find the available energy, and then the latent and sensible heat fluxes were scaled to match the available energy while preserving the Bowen ratio. The total annually averaged adjustments to available energy for Illinois and Oklahoma were 8 and 17 W m^{-2}, respectively. In addition to FLUXNET observations, the seasonal cycles of surface temperature and precipitation were compared to the Climate Research Unit (CRU) Time Series 2.0 (TS2.0) and some aspects of the energy budget were evaluated using the National Aeronautics and Space Administration (NASA) Surface Radiation Budget (SRB) dataset, obtained from the NASA Langley Research Center Atmospheric Science Data Center (available online at http://eosweb.larc.nasa.gov).

4. Design of experiments

RegCM3–IBIS and RegCM3–BATS1e were assessed using 4 years of simulated climate (1996–99) chosen for maximum overlap with FLUXNET observations. Each numerical experiment was initialized 1 April 1994 and allowed to spin up for 21 months. The domain was centered at 40°N, 95°W and spanned 100 points zonally, 60 points meridionally with a horizontal grid spacing of 60 km (Fig. 2). The 40-yr European Centre for Medium-Range Weather Forecasts (ECMWF) Re-Analysis (ERA-40) dataset (Uppala et al. 2005) was used to force the boundaries under the exponential relaxation of Davies and Turner (1977). SSTs were prescribed using the National Oceanic and Atmospheric Administration Optimum Interpolation SST dataset (Reynolds et al. 2002).

In RegCM3–BATS1e, vegetation classes were directly assigned using the Global Land Cover Characterization (GLCC) dataset of the United States Geological Survey (USGS) (United States Geological Survey Center for Earth Resources Observation and Science 1997). In RegCM3–IBIS, the potential global vegetation dataset of Ramankutty (1999) was used to initialize biomes, and then each grid box was populated with plant functional types (PFTs) based on the biome and two datasets: monthly mean climatology of temperature (New et al. 1999) and minimum temperature ever recorded at a location minus the average temperature of the coldest month (P. Bartlein 2000, personal communication). Croplands were then defined in RegCM3–IBIS by the USGS GLCC dataset. In all simulations presented, RegCM3–IBIS was run with static vegetation to create a consistent comparison between models. The vegetative cover (biomes for RegCM3–IBIS, vegetation classes for RegCM3–BATS1e) over each point examined is provided in Table 1. Topography for both models was given by the USGS global 30 arc second elevation dataset (United States Geological Survey Center for Earth Resources Observation and Science 1996) aggregated to a 0.5° × 0.5° spatial resolution.

At initialization, soil temperature was set by the surface temperature boundary condition and soil moisture was assigned based on vegetation type in RegCM3–BATS1e. A global 20-yr 0.5° × 0.5° offline IBIS simulation starting in 1980 was used to initialize soil moisture, soil temperature, and soil ice in RegCM3–IBIS. The monthly mean climatology variables required to run the offline version of IBIS are cloudiness, precipitation rate, relative humidity, temperature, "wet" days per month, near-surface wind speed, and temperature range, which are all products of the Climate Research Unit dataset (New et al. 1999). Differences in the initialization of soil moisture and temperature were shown to be a relatively minor source of variability in the modeling results of similar experiments (Winter et al. 2009).

FLUXNET observations and output from the RegCM3–IBIS and RegCM3–BATS1e simulations were averaged
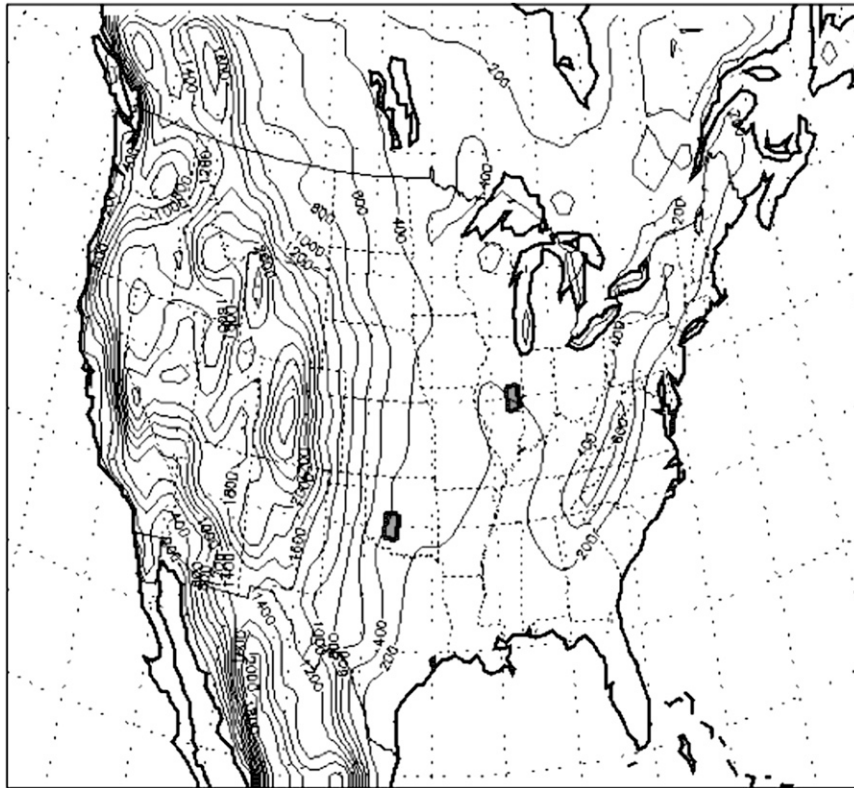
FIG. 2. Domain and topography (m) with, from north to south, $1.0° \times 1.0°$ shaded boxes delineating the extent of spatial averaging over Bondville, IL (right box), and Little Washita Watershed, OK (left box).

to create 6-hourly time series. Saturation vapor pressure was calculated using the empirical formula of Bolton (1980). The slope of the saturation vapor pressure curve was obtained over a 0.2°C increment. FLUXNET relative humidity values were converted to vapor pressure with ERA-40 surface pressure values. Aerodynamic resistance was calculated using the mean canopy wind speed ($\overline{u}$) and the friction velocity (u_*):

$$r_a = \frac{\overline{u}}{u_*^2}. \qquad (7)$$

Surface resistance was computed by solving the Penman–Monteith equation for r_s.

5. Results and discussion

Presented results for both models are $1.0° \times 1.0°$ spatial averages centered over the FLUXNET tower site and are shown in Fig. 2. The top box is centered over Bondville, Illinois, and the bottom box over Little Washita Watershed, Oklahoma. Illinois has temporal coverage for January 1997 through December 1999, while data for the Oklahoma site are available May 1996

to December 1998. Variables from the Illinois and Oklahoma FLUXNET sites are measured at tower top: 8 and 3 m, respectively.

The sensitivity of latent heat flux to available energy was calculated for daylight hours (0700–1900 local time) from May to September, capturing most of the agricultural and natural growing season as well as the increase, peak, and subsequent decline of the seasonal cycle of latent heat flux. Nighttime hours and time intervals with less than 10 W m^{-2} of evapotranspiration were eliminated from the analysis because their contribution to the

TABLE 1. Biomes for RegCM3–IBIS, vegetation classes for RegCM3–BATS1e, over the domain examined ($1.0° \times 1.0°$ boxes shown in Fig. 2). The distribution of biomes–vegetation classes within each box is given by the fraction in parentheses.

	RegCM3–IBIS	RegCM3–BATS1e
Bondville, IL	Cropland (5/6)	Cropland (5/6)
	Savanna (1/6)	Forest field mosaic (1/6)
Little Washita Watershed, OK	Grassland (3/6)	Short grass (3/6)
	Savanna (2/6)	Forest field mosaic (3/6)
	Cropland (1/6)	—

total annual flux of latent heat is minimal. In addition to determining the sensitivity of latent heat flux to available energy using the partial derivative of the Penman–Monteith equation with respect to available energy ("theoretical"), a simple linear regression was also performed to provide an empirical estimate of the response of latent heat flux to changes in available energy ("empirical").

An assessment of the ability of RegCM3–IBIS and RegCM3–BATS1e to simulate the energy and water budgets of each site is presented in section 5a. The theoretical sensitivity of latent heat flux to available energy and the empirical response of latent heat flux to changes in available energy are discussed in section 5b. Finally, the applications of the Penman–Monteith framework are explored in section 5c.

a. Seasonal cycle analysis

Seasonal cycles of shortwave radiation incident at the surface, shortwave radiation absorbed at the surface, latent heat flux, sensible heat flux, 2-m temperature, and precipitation are presented in Figs. 3 and 4 to provide background for the sensitivity analysis and identify errors in model simulations that may propagate through the Penman–Monteith framework. Values for FLUXNET are point measurements averaged over the dates available. Model, CRU TS2.0, and NASA SRB values are $1.0° \times 1.0°$ spatial averages centered over the FLUXNET site for 1996–99.

Both models overestimate shortwave radiation incident at the Illinois site during the summer months (June, July, August) by ≈ 30 W m^{-2}. RegCM3–IBIS also simulates excess radiation throughout much of the year. Over Oklahoma, RegCM3–IBIS and RegCM3–BATS1e simulate some additional shortwave radiation incident when compared to FLUXNET, but are in general agreement NASA SRB. RegCM3–BATS1e overestimates shortwave radiation incident by ≈ 35 W m^{-2} at the Oklahoma site during the month of June. Surface albedos appear relatively consistent across models and observations as errors in shortwave radiation absorbed are well correlated with errors in shortwave radiation incident.

Both models simulate excess latent heat flux during the spring at the Illinois and Oklahoma sites. Summer latent heat flux is overestimated by RegCM3–IBIS, ≈ 25 W m^{-2}, at the Oklahoma site and by RegCM3–BATS1e, ≈ 30 W m^{-2}, over Illinois. Both models miss the early summer reduction of sensible heat flux found in the Illinois FLUXNET observations. RegCM3–IBIS overestimates sensible heat flux at both sites during the summer. Additional sensible heat in RegCM3–IBIS is likely attributable to increased surface temperatures resulting from surplus shortwave radiation incident. RegCM3–BATS1e underestimates

the flux of sensible heat during the spring and fall at the Illinois site. Sensible heat flux values are overestimated by RegCM3–BATS1e at the Oklahoma site by as much as 55 W m^{-2} during the month of June. The coincident decrease of top of the atmosphere (TOA) albedo and surface soil moisture over Oklahoma (not pictured) in RegCM3–BATS1e for the months of June and July suggest a reduction of cloud cover, which contributes to the overestimation of shortwave incident radiation.

Two-meter temperature is well simulated by both models at the Oklahoma site and by RegCM3–BATS1e over Illinois. RegCM3–IBIS has a significant warm bias during the summer at the Illinois site, approximately 2°C, which is likely a result of the overestimation of shortwave radiation incident. The ability of RegCM3–IBIS and RegCM3–BATS1e to accurately simulate the seasonal cycles of precipitation over Illinois and Oklahoma is modest, and there are significant discrepancies between FLUXNET and CRU TS2.0 observations. Generally, both models tend to overestimate precipitation at the Illinois site. Monthly precipitation is highly variable over Oklahoma and there is little agreement between RegCM3–IBIS, RegCM3–BATS1e, FLUXNET, and CRU TS2.0.

Summer 2-m temperature and precipitation were also evaluated throughout the United States using the CRU TS2.0 dataset. Figure 5 shows the average June, July, August 2-m temperature and precipitation biases of RegCM3–IBIS and RegCM3–BATS1e. Two-meter temperature is overestimated by RegCM3–IBIS across much of the United States, with the largest errors occurring along the western and northeastern coasts. RegCM3–BATS1e is a significantly cooler model, with warmer than observed temperatures over the Baja Peninsula and Southern California only. RegCM3–BATS1e simulates a large wet bias along the Gulf of Mexico extending throughout the southeastern United States. In contrast, RegCM3–IBIS underestimates precipitation over the Gulf of Mexico and within Florida.

b. Sensitivity of latent heat flux to available energy

Figure 6 shows the theoretical sensitivity of latent heat flux to available energy and the empirical response of latent heat flux to changes in available energy for each model and FLUXNET observations. Error bars showing one standard deviation are included in the theoretical sensitivity figures and R^2 values that describe the correlation between evapotranspiration and available energy are included in the empirical plots. Some of the annual variations in the theoretical sensitivities of latent heat flux to available energy are reflected in the empirical responses of latent heat flux to changes in available energy; however, in general there is little agreement
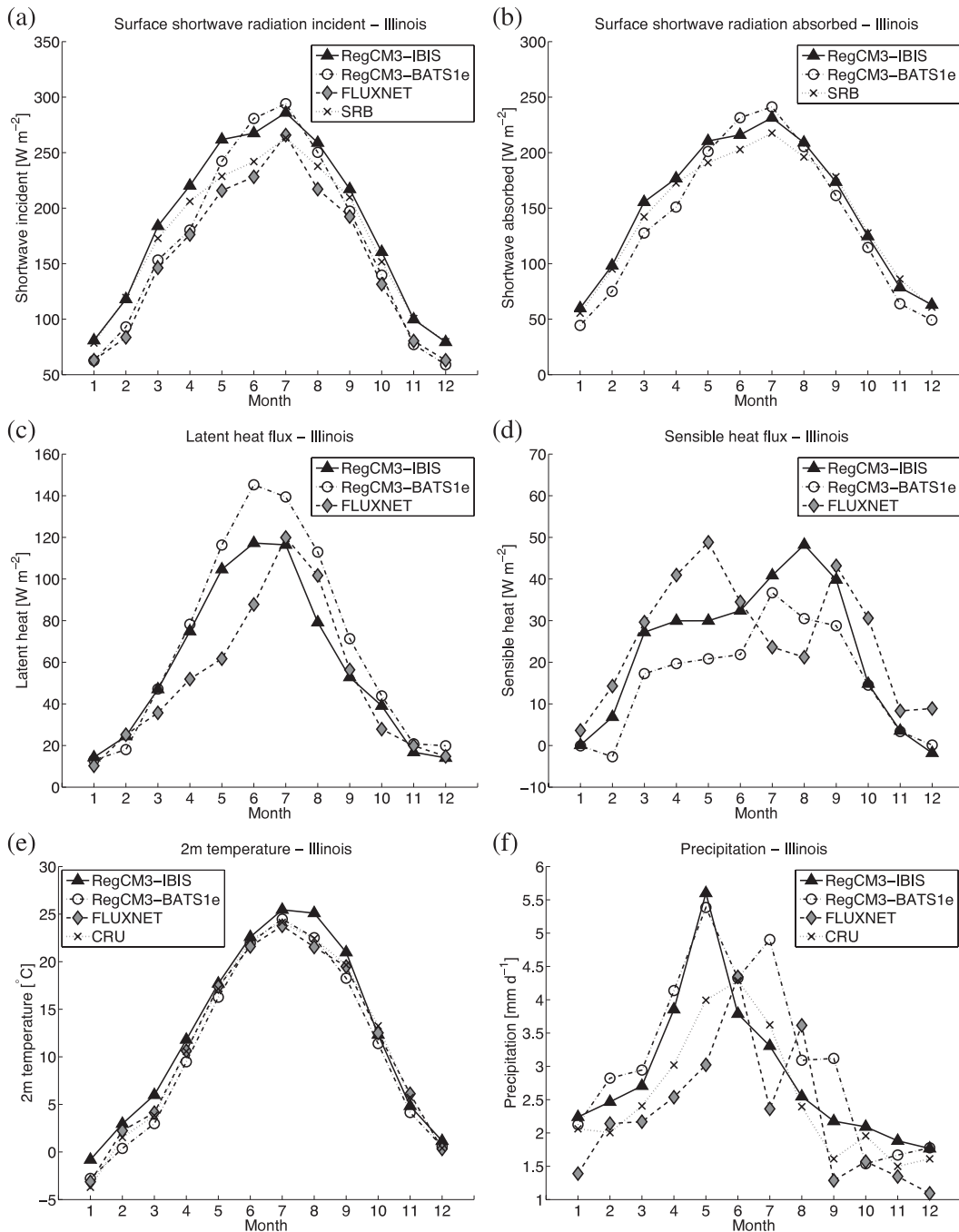
FIG. 3. Seasonal cycles of (a) surface shortwave radiation incident, (b) surface shortwave radiation absorbed, (c) latent heat flux, (d) sensible heat flux, (e) 2-m temperature, and (f) precipitation for Bondville, IL. Each point is a monthly average for the years 1996–99 (FLUXNET 1997–99).

between the two methods. The most noticeable difference is that the theoretical sensitivities are always less than the empirical responses. Discrepancies between the theoretical sensitivity of latent heat flux to available energy and the empirical response of latent heat flux to changes in available energy are due in part to comparing

a partial derivative to an approximation of the full derivative. In the Penman–Monteith framework, all variables except available energy are held constant. This is not true of a regression, which just examines the relationship between a response and explanatory variable, treating the influence of other factors as noise that
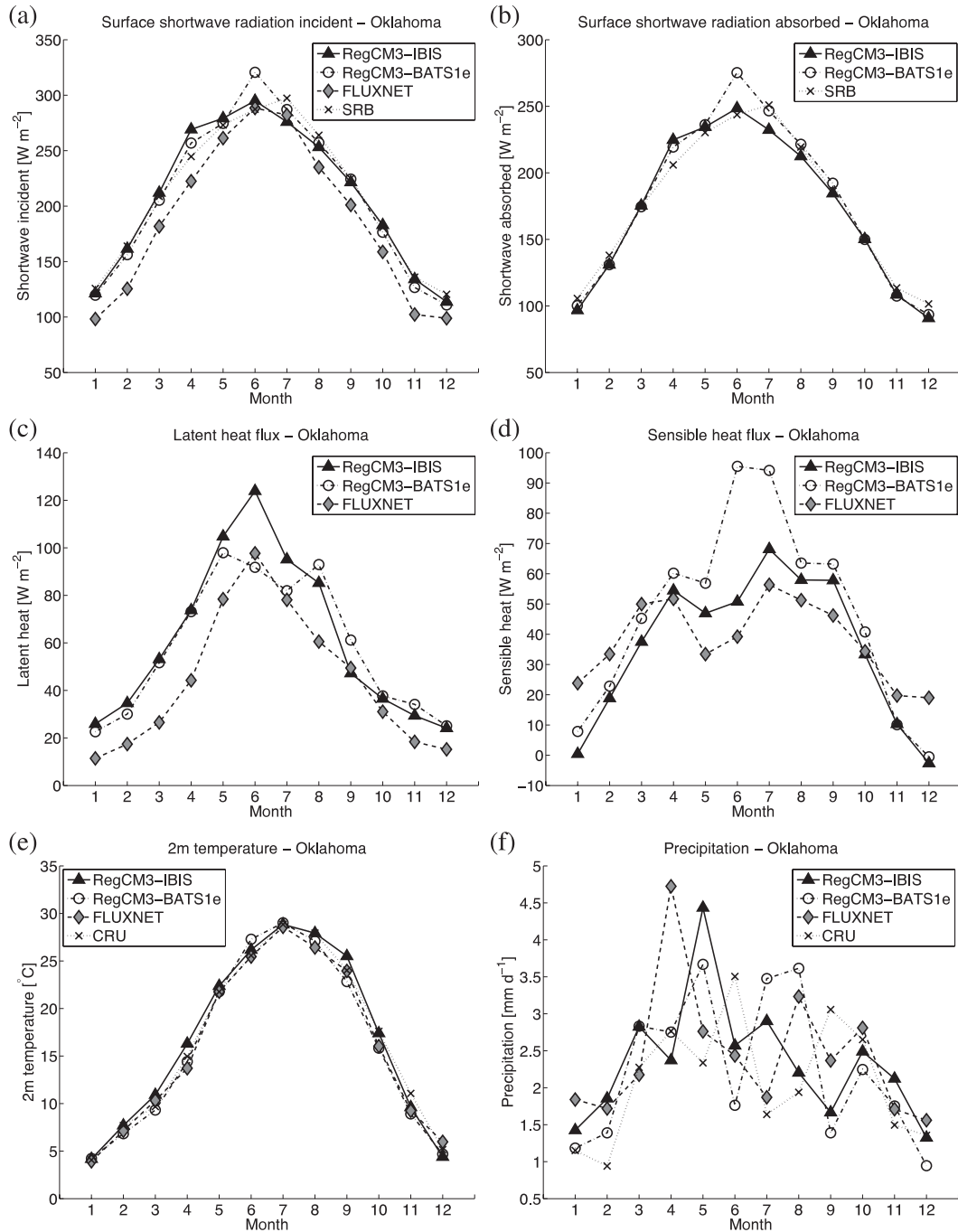
FIG. 4. As in Fig. 3, but for Little Washita Watershed, OK and the years 1996–99 (FLUXNET 1996–98).

degrades the R^2 value. Additional inaccuracies in the theoretical framework may result from applying the Penman–Monteith equation at such fine scales. However, as observational records continue to expand both spatially and temporally, errors in the application of this framework should be reduced.

RegCM3–BATS1e overestimates the theoretical sensitivity of latent heat flux to available energy at the Illinois

site. At this site, RegCM3–IBIS is in agreement with FLUXNET on average, but it overestimates the theoretical sensitivity in May and June and underestimates it in the late summer. The empirical responses of latent heat flux simulated by RegCM3–IBIS and RegCM3–BATS1e over Illinois are too high in the early summer and too low in July, August, and September when compared to FLUXNET. The theoretical sensitivities of both models
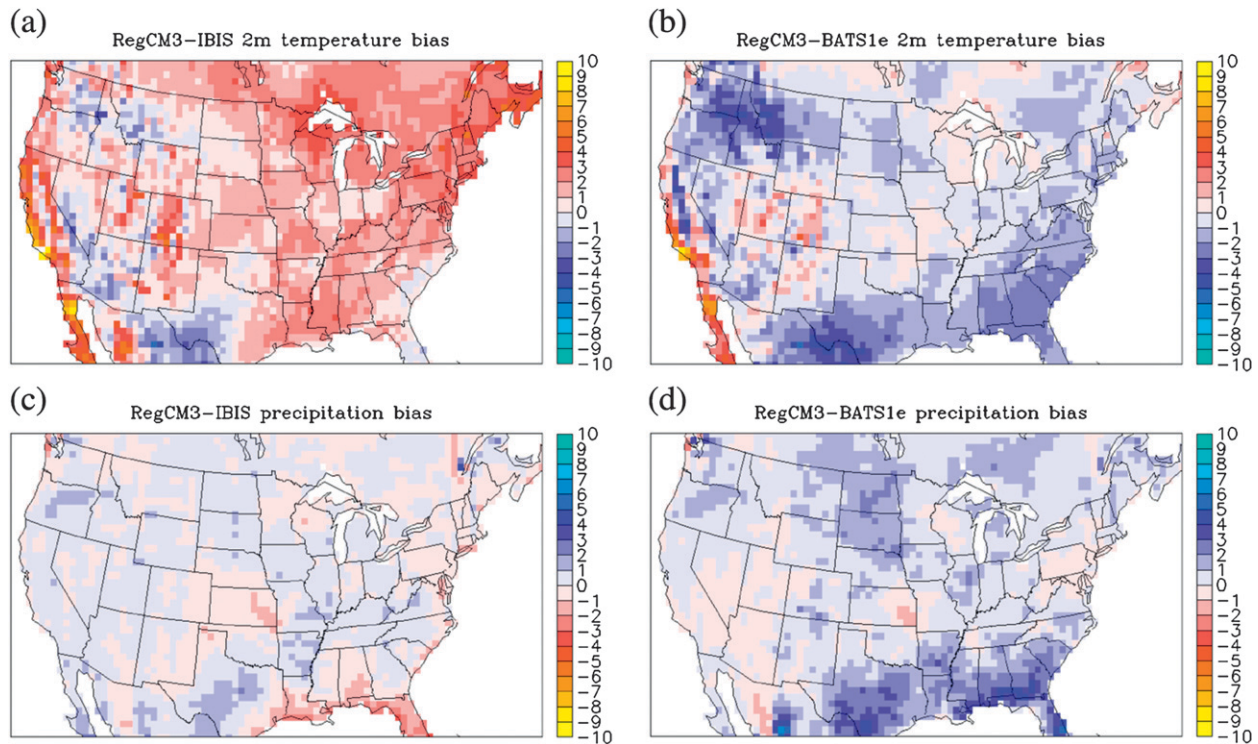
FIG. 5. Average 2-m temperature (°C) and precipitation (mm d^{-1}) biases for (a),(c) RegCM3–IBIS and (b),(d) RegCM3–BATS1e compared to CRU TS2.0 for Jun–Aug 1996–99.

are similar to the observed theoretical sensitivity of latent heat flux to available energy at the Oklahoma site; however, the empirical responses are underestimated by RegCM3–IBIS and RegCM3–BATS1e.

The accumulation of greenhouse gasses (CO_2, CH_4, water vapor, etc.) in the atmosphere increases downward longwave radiation and available energy. Underestimating the sensitivity of latent heat flux to available energy has many potential consequences, including the retention of soil moisture, less water vapor in the canopy, a decrease in plant respiration, increased sensible heat flux, and warmer surface temperatures. This is apparent even in the control simulations, where RegCM3–IBIS underestimates the sensitivity of latent heat flux to available energy during the late summer over Illinois, which coincides with an increase in surface temperature and sensible heat flux. And while the results presented in section 5a demonstrate that the simulation of 2-m temperature is fairly robust despite inaccuracies in latent heat flux, small changes in the simulation of temperature and water vapor could have significant implications for more sensitive variables, such as precipitation and cloudiness. Overestimating the sensitivity of latent heat flux to available energy could also be detrimental to the accuracy of model simulations. Excess latent heat flux will dampen the increase in surface temperature resulting

from additional available energy, introducing a number of biases to the system. Sensitivity experiments are currently being conducted to further evaluate the impacts of changes in available energy on the surface water and energy budgets.

As discussed above, to provide an accurate prediction of future climate, a model must capture both the correct climatology of evapotranspiration and the correct sensitivity of latent heat flux to available energy. Models with a higher climatology of latent heat flux will likely have a higher sensitivity based solely on the magnitude of the fluxes involved. To address this bias, Fig. 7 shows the theoretical sensitivity of latent heat flux to available energy and the empirical response of latent heat flux to changes in available energy normalized by the latent heat flux, integrating the climatology of evapotranspiration and the theoretical sensitivity–empirical response of latent heat flux into a single seasonal cycle. The normalized theoretical sensitivities of latent heat flux to available energy and empirical responses of latent heat flux to changes in available energy of FLUXNET observations are largest, a result of the relatively low values of latent heat in the FLUXNET dataset. RegCM3–BATS1e simulates high values of evapotranspiration, resulting in reduced normalized theoretical sensitivities and empirical responses when compared to RegCM3–IBIS and FLUXNET.
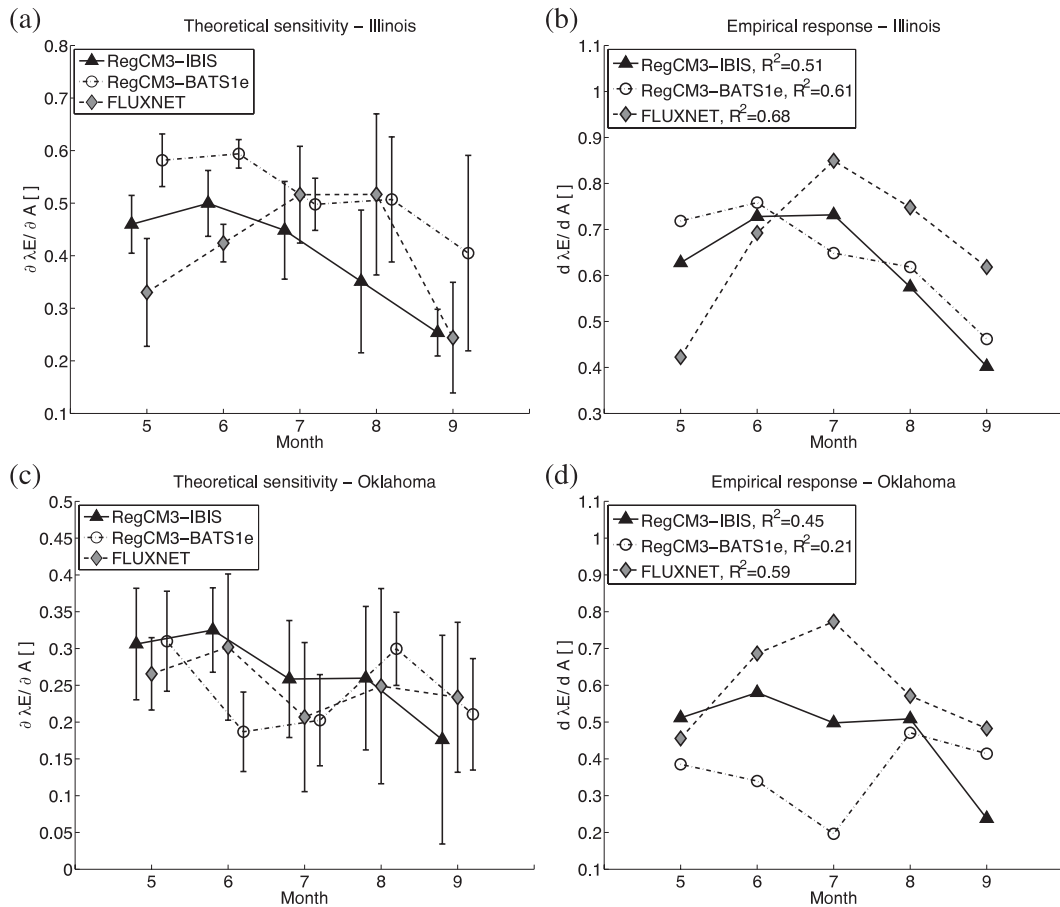
FIG. 6. (a),(c) Theoretical sensitivity with error bars denoting 1 standard deviation from the mean and (b),(d) empirical response with associated R^2 values. Each point is a monthly average for the years 1996–99 (FLUXNET 1997–99 for Illinois, 1996–98 for Oklahoma).

c. Applying the Penman–Monteith framework

One benefit of using the Penman–Monteith framework to calculate the sensitivity of latent heat flux to available energy is the additional analyses possible. The empirical response of latent heat flux to changes in available energy, derived from a regression, can at best show correlation. It addresses nothing beyond the variables considered nor provides any causal information. Using the Penman–Monteith equation is a mechanistic approach that allows examination at every level. Equation (5) shows that the theoretical sensitivity of latent heat flux to available energy is a function of the ratio of surface resistance to aerodynamic resistance. While Δ is also variable, it remains relatively constant over the months considered.

The surface and aerodynamic resistances for both models are presented in Fig. 8. Combined with Eq. (5), these plots explain many of the differences illustrated in Fig. 6. The increase in the surface resistance of RegCM3–IBIS at the end of the summer over Illinois and Oklahoma

increases the denominator of Eq. (5), thus reducing the sensitivity of latent heat flux to available energy in RegCM3–IBIS. This suggests an error within the model, as large values of surface resistance are not found in the FLUXNET observations. Aerodynamic resistance also plays an important role in the sensitivity of latent heat flux to available energy. RegCM3–IBIS simulates high values of aerodynamic resistance at both sites, reducing the denominator of Eq. (5) and increasing the sensitivity of the model.

In addition to assessing the sensitivity of latent heat flux to available energy, the ratio of surface resistance to aerodynamic resistance can also be used to provide information about the climatology of evapotranspiration. For example, RegCM3–BATS1e is expected to simulate large values of latent heat flux over Illinois because of its low surface resistance. In contrast, the higher values of surface resistance in RegCM3–BATS1e at the Oklahoma site should result in lower evapotranspiration. Both are observed, as evidenced in Figs. 3 and 4.
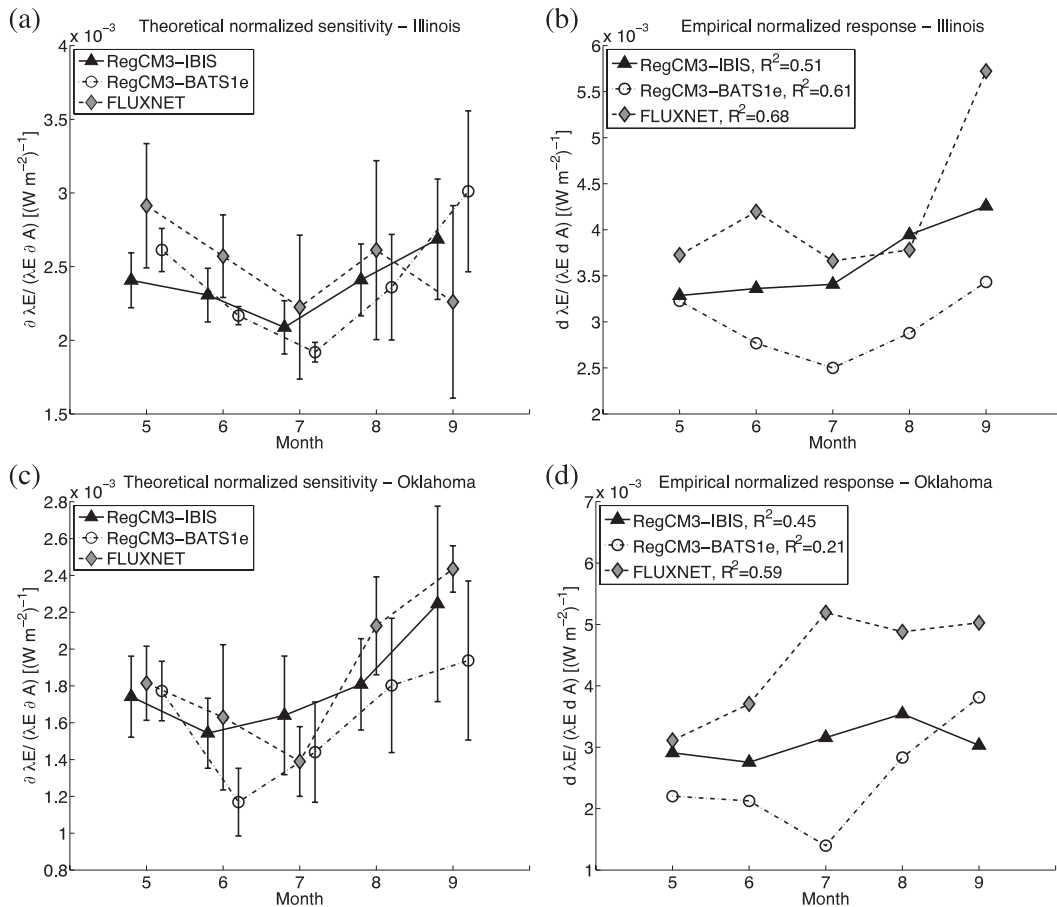
FIG. 7. As in Fig. 6, but for theoretical normalized sensitivity and empirical normalized response.

Figure 9 is exactly the same as Fig. 1 but includes the approximate position of RegCM3–IBIS, RegCM3–BATS1e, and FLUXNET during the summer at the Illinois site. RegCM3–IBIS simulates high surface resistance and relatively low values of latent heat flux. In contrast, low values of surface resistance in RegCM3–BATS1e promote increased fluxes latent heat and an increased sensitivity of evapotranspiration to available energy.

The natural extension of using the Penman–Monteith framework to evaluate disparities between models and observations is applying it to guide improvements. The normalized sensitivity of latent heat flux to available energy is underestimated by both models over Illinois, but the reason why differs. The surface resistance of RegCM3–IBIS is too high. This suggests that there needs to be a reduction of the controls on evapotranspiration. In RegCM3–IBIS, the surface resistance is a function of the photosynthetic rate, CO_2 concentration, and water vapor concentration. Each factor should be examined to see which is limiting, and that limiting factor should be assessed and revised if appropriate. RegCM3–BATS1e

simulates low values of surface resistance and aerodynamic resistance, causing an overestimation of latent heat flux and thus reducing the normalized sensitivity. In this case, each component of the resistance formulas in BATS1e—solar radiation, saturation vapor pressure, seasonal temperature, soil moisture, and wind speed—should be evaluated. It is important to note that errors in the energy budget must be fixed in conjunction with those in the surface physics scheme, as the accuracy of a simulation depends both on the correct flux of radiation into the system and the correct partitioning of that energy.

6. Conclusion

A thorough comparison of RegCM3–IBIS, RegCM3–BATS1e, and FLUXNET observations is presented. In addition to examining the climatology of energy and water fluxes, a framework using the Penman–Monteith equation was developed to assess the theoretical sensitivity of latent heat flux to available energy. An empirical estimate of the response of latent heat flux to changes in available energy was calculated by regression. The
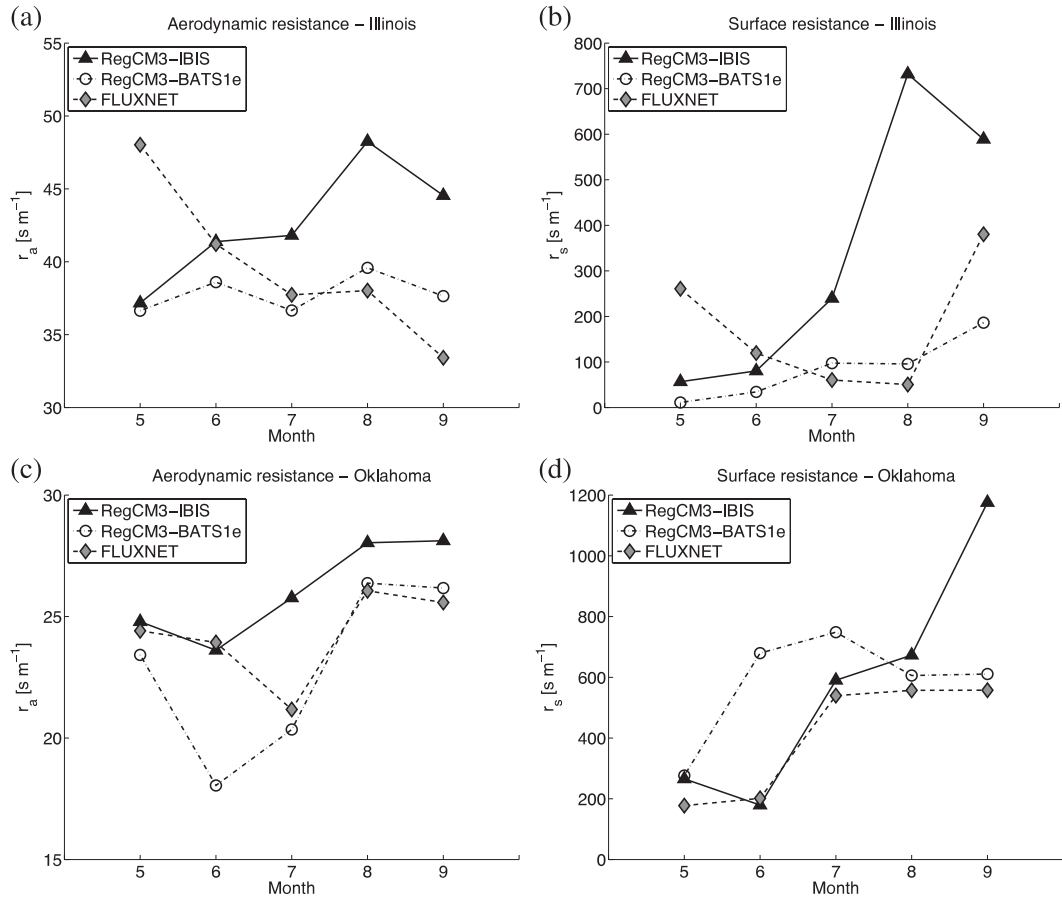
FIG. 8. (a),(c) Aerodynamic resistance and (b),(d) surface resistance. Each point is a monthly average for the years 1996–99 (FLUXNET 1997–99 for Illinois, 1996–98 for Oklahoma).

theoretical and empirical values show limited agreement, with some differences attributable to comparing a partial derivative to an approximation of the full derivative.

The advantage of using the Penman–Monteith framework is the ability to expose relationships beyond a simple correlation. The physical basis of the Penman–Monteith equation makes it possible to tell not only if but exactly where models differ. In addition, completing extensive assessments that reveal the mechanics of each model ensures that skillful simulations are the result of an accurate model, as opposed to merely getting the right answer for the wrong reason. Information derived from this analysis is also valuable for correcting errors in parameterizations. It is expected that a comparison of models with less in common (different spatial resolutions, atmospheric representations, etc.) would yield more disparate sensitivities of latent heat flux to available energy and greater insight.

RegCM3–IBIS and RegCM3–BATS1e do a reasonable job of simulating the theoretical sensitivity of latent heat flux to available energy on average over the summer; however, there are significant differences between the seasonal cycles of both models and FLUXNET observations. RegCM3–IBIS and RegCM3–BATS1e underestimate the normalized sensitivity of latent heat flux to available energy. The empirical responses of latent heat
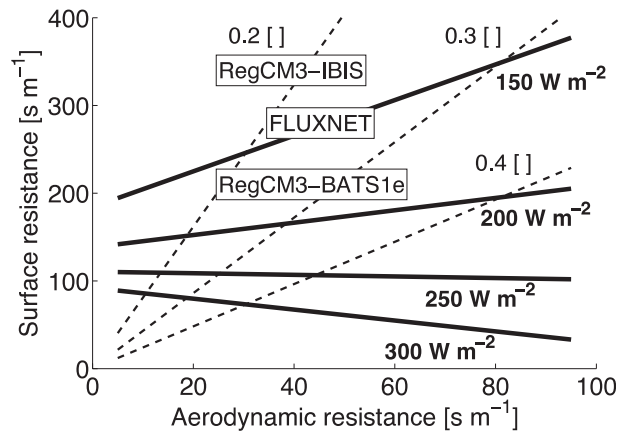

FIG. 9. As in Fig. 1, but also showing the approximate positions of RegCM3–IBIS, RegCM3–BATS1e, and FLUXNET during the summer at the Illinois site.

flux to changes in available energy are generally greater than the theoretical sensitivities of latent heat flux to available energy derived from the Penman–Monteith framework. Both models underestimate the response of latent heat flux to changes in available energy when compared to FLUXNET using the empirical method. This damped response of latent heat flux to an increase in the radiative forcing will have a substantial effect on the energy balance. Energy not partitioned to latent heat must leave the system as sensible heat. This would likely result in an overestimation of temperature and an exacerbation of temperature-dependent feedbacks in climate change simulations.

Ideally, models would be verified by comparing the state of the model to a past observed state; however, only a very small subset of state observations is available. Simple, intuitive equations can be leveraged to reveal a more complete picture of simulated and observed climate, expanding the scope of parameterization assessment and ultimately improving our ability to model the earth system.

REFERENCES

Baldocchi, D., and Coauthors, 2001: FLUXNET: A new tool to study the temporal and spatial variability of ecosystem-scale carbon dioxide, water vapor, and energy flux densities. *Bull. Amer. Meteor. Soc.,* **82,** 2415–2434.

Bolton, D., 1980: The computation of equivalent potential temperature. *Mon. Wea. Rev.,* **108,** 1046–1053.

Collins, W. D., J. M. Lee-Taylor, D. P. Edwards, and G. L. Francis, 2006: Effects of increased near-infrared absorption by water vapor on the climate system. *J. Geophys. Res.,* **111,** D18109, doi:10.1029/2005JD006796.

Davies, H., and R. Turner, 1977: Updating prediction models by dynamical relaxation: An examination of the technique. *Quart. J. Roy. Meteor. Soc.,* **103,** 225–245.

Falge, E., and Coauthors, cited 2005: Fluxnet Marconi conference gap-filled flux and meteorology data, 1992–2000. [Available online at http://www.daac.ornl.gov.]

Foley, J., I. Prentice, N. Ramankutty, S. Levis, D. Pollard, S. Sitch, and A. Haxeltine, 1996: An integrated biosphere model of land surface processes, terrestrial carbon balance, and vegetation dynamics. *Global Biogeochem. Cycles,* **10,** 603–628.

Kucharik, C., and K. Brye, 2003: Integrated Biosphere Simulator (IBIS) yield and nitrate loss predictions for Wisconsin maize receiving varied amounts of nitrogen fertilizer. *J. Environ. Qual.,* **32,** 247–268.

New, M., M. Hulme, and P. D. Jones, 1999: Representing twentieth-century space–time climate variability. Part I: Development of a 1961–90 mean monthly terrestrial climatology. *J. Climate,* **12,** 829–856.

Pal, J. S., and Coauthors, 2007: Regional climate modeling for the developing world: The ICTP RegCM3 and RegCNET. *Bull. Amer. Meteor. Soc.,* **88,** 1395–1409.

Ramankutty, N., 1999: Estimating historical changes in land cover: North American croplands from 1850 to 1992. *Global Ecol. Biogeogr.,* **8,** 381–396.

Reynolds, R. W., N. A. Rayner, T. M. Smith, D. C. Stokes, and W. Wang, 2002: An improved in situ and satellite SST analysis for climate. *J. Climate,* **15,** 1609–1625.

Shuttleworth, W., 1979: Evaporation. Tech. Rep. 56, Institute of Hydrology, 63 pp.

Twine, T. E., and Coauthors, 2000: Correcting eddy-covariance flux underestimates over a grassland. *Agric. For. Meteor.,* **103,** 279–300.

United States Geological Survey Center for Earth Resources Observation and Science, cited 1996: Global 30 arc second elevation dataset (GTOPO30). [Available online at http://eros.usgs.gov/#/Find_Data/Products_and_Data_Available/gtopo30_info.]

——, cited 1997: Global land cover characterization. [Available online at http://edc2.usgs.gov/glcc/glcc.php.]

Uppala, S. M., and Coauthors, 2005: The ERA-40 Re-Analysis. *Quart. J. Roy. Meteor. Soc.,* **131,** 2961–3012.

Winter, J. M., J. S. Pal, and E. A. B. Eltahir, 2009: Coupling of Integrated Biosphere Simulator to Regional Climate Model version 3. *J. Climate,* **22,** 2743–2757.